Analyst

PAPER

View Article Online
View Journal | View Issue

Cite this: *Analyst*, 2016, **141**, 2896

Spectrochemical analysis of sycamore (*Acer pseudoplatanus*) leaves for environmental health monitoring†

James Ord,[a,b] Holly J. Butler,[b] Martin R. McAinsh*[b] and Francis L. Martin*[b,c]

Terrestrial plants are ideal sentinels of environmental pollution, due to their sedentary nature, abundance and sensitivity to atmospheric changes. However, reliable and sensitive biomarkers of exposure have hitherto been difficult to characterise. Biospectroscopy offers a novel approach to the derivation of biomarkers in the form of discrete molecular alterations detectable within a biochemical fingerprint. We investigated the application of this approach for the identification of biomarkers for pollution exposure using the common sycamore (*Acer pseudoplatanus*) as a sentinel species. Attenuated total reflection Fourier-transform infrared (ATR-FTIR) spectroscopy was used to interrogate leaf tissue collected from three sites exposed to different levels of vehicle exhaust emissions. Following multivariate analysis of acquired spectra, significant biochemical alterations were detected between comparable leaves from different sites that may constitute putative biomarkers for pollution-induced stress. These included differences in carbohydrate and nucleic acid conformations, which may be indicative of sub-lethal exposure effects. We also observed several corresponding spectral alterations in both the leaves of *A. pseudoplatanus* exposed to ozone pollution under controlled environmental conditions and in leaves infected with the fungal pathogen *Rhytisma acerinum*, indicating that some stress-induced changes are conserved between different stress signatures. These similarities may be indicative of stress-induced reactive oxygen species (ROS) generation, although further work is needed to verify the precise identity of infrared biomarkers and to identify those that are specific to pollution exposure. Taken together, our data clearly demonstrate that biospectroscopy presents an effective toolkit for the utilisation of higher plants, such as *A. pseudoplatanus*, as sentinels of environmental pollution.

Received 16th February 2016,
Accepted 6th April 2016

DOI: 10.1039/c6an00392c

www.rsc.org/analyst

1. Introduction

Exposure to complex mixtures of anthropogenic emissions in the environment is currently a major concern for human health. Air pollution from industrial and vehicular sources has been linked with respiratory illness, cardiovascular disease, cancer, and mortality.[1] Although gaseous pollutants (*e.g.*, SO_2) have been of major concern throughout the last century,[2] attention has since shifted to other potentially dangerous pollutants, notably particulate matter (PM_{10} and $PM_{2.5}$),[3] nanoparticles,[4] and polycyclic aromatic hydrocarbons (PAHs).[5] While the adverse effects of individual agents are well-studied, the effects of exposure to mixtures may be difficult to predict, and thus there is an urgent need to monitor environmental exposures in sentinel organisms.[6,7]

The advantages of using higher plants as sentinels for environmental pollution are well known.[8,9] Firstly, as sedentary organisms, they allow easy comparison between set geographical locations. Furthermore, plant biochemistry is fundamentally similar to that of animals in aspects relevant to toxic exposure, including DNA organisation and repair mechanisms, and antioxidant activity.[10] Plant cells can be exposed to air pollutants either directly *via* leaf stomata, or indirectly *via* root uptake of pollutants deposited in the soil. Adverse effects on plants can be induced by a variety of air pollutants, among which ozone (O_3) is considered to be the most damaging. O_3 causes oxidative damage to cell components *via* the formation of reactive oxygen species (ROS),[11] which are also generated by exposure to heavy metals.[12] Other adverse effects of air

[a]*Department of Animal and Plant Sciences, University of Sheffield, Sheffield S10 2TN, UK*
[b]*Centre for Biophotonics, Lancaster Environment Centre, Lancaster University, Lancaster LA1 4YQ, UK. E-mail: f.martin@lancaster.ac.uk, m.mcainsh@lancaster.ac.uk*
[c]*School of Pharmacy and Biomedical Sciences, University of Central Lancashire, Preston PR1 2HE, UK*

†Electronic supplementary information (ESI) available. See DOI: 10.1039/c6an00392c

pollutants on plant cells may include acidification of the intracellular space by SO_2,[11] and genotoxicity of nanoparticles[13] and PAHs.[14]

For a plant species to be utilised as a sentinel requires that it is present in areas of both high and low pollution exposure, and that it also exhibits quantifiable biomarkers for the adverse effects of pollution. The deciduous tree *Acer pseudoplatanus* (common sycamore) represents an ideal sentinel species, due to its widespread European distribution, and frequent occurrence in urban and rural areas. Previous attempts to utilise *A. pseudoplatanus* as a sentinel have relied on the abundance of tar spot (*Rhytisma acerinum*) fungal lesions (stromata) on leaf surfaces, as the fungus was perceived to be sensitive to SO_2 exposure.[15] However, this has since been refuted, due to evidence that the prevalence of the fungus in urban areas is reduced by leaf litter clearance.[16]

A range of approaches have been used for the detection of environmental stress biomarkers in higher plants, including chlorophyll fluorescence measurement for effects on photosynthetic efficiency,[17] and gas chromatography for examining changes in leaf fatty acid composition in response to metal exposure.[18] The *Tradescantia* micronucleus (Trad-MCN) assay, which uses the appearance of micronuclei in tetrad phase pollen cells of *Tradescantia* spp. as a biomarker of chromosomal anomalies, has also been widely used to study genotoxicity.[19] There are disadvantages inherent in many of the existing biomarker systems used in plant toxicology: (i) they rely on a single endpoint, and do not account for the wide range of biochemical effects that may be exerted by pollutants; and, (ii) they may require extensive sample preparation.[18] Hence, development of informative, non-destructive, and high-throughput approaches for the identification of robust biomarkers for environmental stress is essential.

Biospectroscopy refers to the application of vibrational spectroscopy techniques to address biological questions.[20,21] As such, it offers a novel approach to biomarker derivation which is both sensitive and high-throughput, and which can be used to deduce a wide range of effects within a biochemical 'fingerprint'.[22] Infrared (IR) spectroscopy relies upon the absorption of IR at different wavelengths by the principle functional groups, which constitute molecular components of cells depending on the vibrations generated by their chemical bonds.[23] Attenuated total reflection Fourier-transform infrared (ATR-FTIR) spectroscopy employs a diamond crystal, through which an IR beam is transmitted and penetrates a few microns into the sample. Consequently, the reflected beam delivers an absorbance spectrum with distinct wavenumber peaks corresponding to biological molecules present including amides, nucleic acids, and polysaccharides.[24] The resulting datasets are complex, requiring computational analyses of the spectra in order to determine the distinguishing features between experimental treatments.[20,25] Multivariate techniques such as principal component analysis-linear discriminant analysis (PCA-LDA) are typically performed to achieve this.

Biochemical fingerprints derived from ATR-FTIR have strong potential to reflect changes induced by exposure to xenobiotics and therefore biospectroscopy is increasingly being utilised in ecotoxicology, with toxic effects having been characterised *in vitro*,[26,27] and in sentinel organisms such as birds,[28] earthworms,[29] catfish, and water spinach.[30] Given the advantages of plants as sentinels, biospectroscopy offers the potential of a convenient plant-based monitoring system for pollution exposure over time and space. This technique is ideal for analysing plant tissue, as it requires little-to-no sample preparation, allowing specimens to be collected from the field and analysed rapidly.[21,31]

Plants are exposed to a range of environmental stresses, both abiotic and biotic, that will act together to affect their biochemical fingerprint and which may confound attempts to study pollution-induced alterations. Most notably, plant pathogens represent a ubiquitous biotic stress in the environment. Pathogens of *A. pseudoplatanus* include the tar spot leaf fungus (*Rhytisma acerinum*),[16] and leaf galls induced by the mite *Artacris macrorhynchus*.[32] The presence of these pathogens or the plant's defensive response may substantially alter leaf biochemistry, and therefore it is essential to assess their impacts on the biochemical fingerprint of *A. pseudoplatanus* if it is to be considered as a candidate as a sentinel species for environmental pollution monitoring.

Herein, the potential of *A. pseudoplatanus* as a sentinel for environmental exposure was assessed using biospectroscopy. Specifically, the effects of different pollution scenarios on the biochemical fingerprints of field-derived leaf samples were examined, with the aim of identifying spectral biomarkers associated with pollution exposure. Additionally, we examined the effects of O_3 fumigation on leaves of *A. pseudoplatanus* under controlled environment conditions and *R. acerinum* infection on the derived biochemical fingerprints. We show that there are key spectral differences between *A. pseudoplatanus* leaves sampled from environments with different pollution exposures, which are indicative of plant stress and which, importantly, could not be detected using changes in chlorophyll fluorescence (Fv/Fm). If these alterations can be established to provide definitive and robust biomarkers of pollution-induced stress this will confirm *A. pseudoplatanus* as a sentinel plant system providing an effective approach to environmental health monitoring.

2. Materials and methods

Field sites

Three field sites were selected, representing a range of exposure levels to environmental pollutants (Table 1). All three sites featured an abundance of mature *A. pseudoplatanus*. Site 1 comprised an area of rural woodland within the Fairfield Nature Reserve, Lancaster (UK). The site is 1.2 km from the nearest busy road, and is further shielded from busy roads by rows of trees and a canal. Site 2 is an area of mixed vegetation located immediately adjacent to a busy 6-lane highway. Site 3 is an urban site located on a busy city centre roundabout. In addition, a fourth site (Site 4) was used to study the

Table 1 Descriptions of the three main study sites from which *A. pseudoplatanus* samples were taken for the comparison of different pollution scenarios

Site	Pollution exposure	Site description
Site 1	Rural (reference site)	A woodland area in the Fairfield Nature Reserve, Lancaster. The site is not immediately exposed to pollution sources such as busy roads. The *A. pseudoplatanus* trees at the site were planted in the 1830s.
Site 2	Highway	A woodland area at the edge of Lancaster University campus, and next to a busy 6-lane highway. This was the most densely vegetated site, featuring a very high abundance of *A. pseudoplatanus*.
Site 3	Urban	A busy roundabout near Lancaster's urban centre, frequently used by vehicles. Several mature *A. pseudoplatanus* trees were identified at the site, including three on the roundabout itself.

effects of *R. acerinum* infection. This was comprised of abundant *A. pseudoplatanus* vegetation in hedges bordering a rural road only infrequently used by light road vehicles.

Sample collection and storage

A pilot study was undertaken to determine the method for sample storage. We compared the spectral signatures of leaves maintained in a moist condition[31] and leaves fixed in 70% ethanol (three immersion times: 10 min, 30 min, and 60 min) after 24 h, with the spectral signature of moist leaves on the day of collection. Ethanol fixation induced a significant shift in LD1 scores, which increased with immersion time, whereas there was no significant effect of the moist condition after 24 h [see ESI Fig. S1†].

Leaves (physiological age ≤3 months) were removed from mature *A. pseudoplatanus* trees (age unknown) by cutting the petiole no less than 1 cm from the leaf and placing them in zip-lock bags containing 3× damp cotton wool balls to prevent desiccation.[31] For Sites 1–3, three leaves were collected from each of five trees (15 total leaves) from low in the canopy, approximately 1–3 m from the ground. We selected young leaves which fell within 5–10 cm in width, and did not display any obvious signs of foliar disease (*e.g.*, herbivory, tar spots) or senescence (*e.g.*, chlorosis, desiccation). After transport to the laboratory, leaves were rinsed in reverse osmosis water to remove insects and mites, and placed on dry paper towels to remove excess water. Spectral acquisition followed immediately, with five spectra taken per leaf sample. The entire study was carried out over three days, one site per day.

Chlorophyll fluorescence measurements

In situ measurements of the ratio of variable to maximal fluorescence of photosystem II (Fv/Fm) were taken using a Hansatech Pocket PEA Chlorophyll fluorometer (Hansatech Instruments, Norfolk, UK); Fv/Fm values less than 0.83 are indicative of stress.[17] Three leaves on at least five trees at each site were dark acclimatised for 30–40 min before Fv/Fm values were recorded.

O_3 fumigation

Six cuttings of *A. pseudoplatanus* approximately 20 cm in length comprising of 3–4 healthy leaves were obtained from an additional urban site. In contrast to Site 3, this was located away from busy roads and sheltered from any potential sources of vehicle-derived pollution by high walls. Cuttings were incubated in 500 ml plastic bottles wrapped in aluminium foil to exclude light containing 250 ml of 1 : 1 Hoagland's nutrient solution[33] for 2 days prior to fumigation treatments. Two cuttings each were fumigated with either O_3-free air filtered through Purafil (control) or a modulated episodic ozone treatment (150 ppb or 300 ppb O_3) under the same conditions for a period of three days to simulate a summer O_3 'episode'.[34] In all experiments fumigations were performed at midday although the duration of the fumigation treatment (approximately 6 hours into the photoperiod) varied: day-1 – 2 h, day-2 – 3 h, day-3 – 2 h. Cuttings were then incubated for a further 1-day under the same conditions following fumigation before analysis with ATR-FTIR spectroscopy.

Characterisation of *R. acerinum* infection levels

The severity of *R. acerinum* infection was assessed through the occurrence of characteristic large black lesions, called stromata or tar spots on the adaxial leaf surface. Leaves, 7–9 cm in width, collected from Site 4 were categorised according to the number of tar spots present: category 1 – leaves with no obvious tar spots (control), category 2 – leaves displaying 1–5 obvious tar spots, and Category 3 – leaves displaying ≥10 obvious tar spots. For each category, five leaves were taken from different plants. For each leaf, three spectra were taken from areas of healthy-looking tissue in close proximity to the afflicted area. A second biotic stress, galls induced by the mite, *Artacris macrorhynchus* (protruding red lesions on the adaxial leaf surface) was also examined. In this instance, five leaves displaying prominent galls were collected from the rural Site 1, and were compared with leaves displaying no obvious signs of *A. macrorhynchus*-induced damage taken from the same site as a control. Three spectra were acquired from each leaf, from areas of healthy tissue in close proximity to the affected area or from an equivalent area in the control leaves.

ATR-FTIR spectroscopy

Spectra were acquired from adaxial leaf surfaces using a Bruker Tensor 27 FTIR spectrometer with Helios ATR attachment (Bruker Optics Ltd, Coventry, UK), controlled using the software 'OPUS'. Leaf samples were placed on Low-E slides on the sampling platform, and 1 kg of force was applied for even contact between the crystal and the sample. In between sample spectra, the crystal was cleaned with dH_2O, and background spectra were taken to compensate for atmospheric changes.

Pre-processing and computational analyses

Spectral datasets were classed in Microsoft Excel, and were processed using the IRootLab toolbox (http://irootlab.googlecode.com) running on MATLAB r2013a (The Maths Works Inc., USA). Spectra were pre-processed by cutting to the bio-fingerprint region (1800–900 cm^{-1}), rubberband baseline-corrected, and vector normalised. Pre-processed spectral datasets were analysed by principal component analysis-linear discriminant analysis (PCA-LDA). PCA-LDA is a composite technique whereby PCA is applied to a dataset to reduce the number of variables, then LDA derives orthogonal variables from which between-class variance is maximised over within-class variance.[20] The PCA-LDA models were then used to derive cluster vector plots, derived by pointing from the mean of the control class towards the mean of each treatments class, deriving a separate vector or 'pseudospectrum' for each treatment class, representing biochemical alterations in relation to the control (expressed as coefficient).[25] For more detailed overviews of the computational methods applied in biospectroscopy, readers are directed to the literature.[20,25]

Statistical analyses

All statistical tests were carried out in 'R' version 3.2.3 (R Foundation for Statistical Computing, Austria). To derive values of statistical significance between sites, the first two linear discriminant (LD) scores derived from PCA-LDA were compared using a nested linear mixed effects model fit by REML (Residual Maximum Likelihood) using the (nlme) package (http://CRAN.R-project.org/package=nlme), with 'Tree' and 'Leaf' included as nested random factors to account for variation between individual trees and leaves. Linear mixed effects models with 'Leaf' as a random factor were carried out to assess the significance of shifts in LD scores as a function of O_3 concentration or tar spot number. One-way ANOVA with type-1 sums of squares was used to compare Fv/Fm values between sites. A P-value of <0.05 was considered statistically significant.

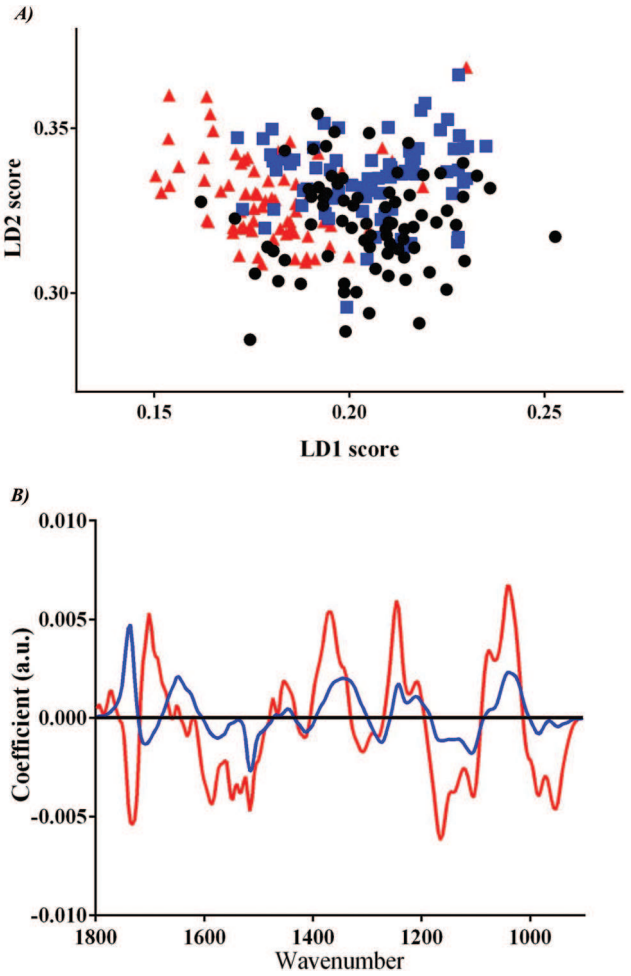

Fig. 1 (A) PCA-LDA scores plot in two dimensions derived from *A. pseudoplatanus* leaf tissue collected from three field sites (black, Site 1; blue, Site 2; red, Site 3) characteristic of different environmental exposures. (B) Cluster vectors plot by PCA-LDA indicating wavenumber basis for segregation between *A. pseudoplatanus* leaf tissue samples collected from three field sites. The two sites exposed to vehicular pollution (blue, Site 2; red, Site 3) were compared to the rural control site (black, Site 1), with the magnitude of the cluster vector peak or trough proportional to the extent of biochemical alteration compared to Site 1.

3. Results and discussion

Site location has a marked impact on the spectral signature of *A. pseudoplatanus*

Spectral datasets from *A. pseudoplatanus* leaves derived from Sites 1–3 were compared using multivariate analyses in order to derive biomarkers of inter-site differences. Following PCA-LDA transformation of pre-processed datasets, the corresponding 2-D LDA scores plot (Fig. 1a) showed a degree of segregation of data from the sites into three clusters, although complete segregation was not observed. A nested linear mixed effects model fit by REML revealed an overall significant effect of site on LD scores ($P = 0.003$), with a significant difference in overall LD scores between the urban-located Site 3 and the rural-located Site 1 ($P = 0.015$). There was no significant difference in overall LD scores between Site 1 and the highway-located Site 2 ($P = 0.158$), but a highly significant difference in LD2 scores ($P = 0.006$).

The pseudospectra shown in the cluster vectors plot (Fig. 1b) displayed substantial changes between sites across the biochemical fingerprint region. Site 2 and Site 3 leaves exhibited several common areas of segregation from Site 1 leaves, suggesting pollution-associated alterations stemming from their different exposures to vehicle exhaust emissions. Several alterations were linked with specific molecular features (Table 2). Notably, alterations in the carbohydrate region (*e.g.*, 1107 cm^{-1} in Site 2, 1165 cm^{-1} in Site 3) may imply alterations to cell wall conformation, reduced photosynthetic capacity, or increased energy expenditure. Alterations were also observed in the DNA/RNA region (~950 cm^{-1}) at both sites, which may suggest exposure to genotoxic agents.[14,35] In addition, peaks

Table 2 ATR-FTIR spectroscopy distinguishing wavenumbers as shown in cluster vectors plot for *A. pseudoplatanus* leaf tissue collected from three field sites characteristic of different environmental exposures to vehicular pollution. For Site 2 and Site 3 leaves, the most important wavenumbers responsible for segregation from control (Site 1) leaves are shown, along with their tentative chemical assignments

Site	Wavenumber (cm^{-1})	Tentative assignment(s)	Reference (s)
Site 2	1736	Lipid; fatty acid esters	(1)
	1647	Amide I; pectin	(1), (3)
	1574	Amide I	
	1516[b]	Amide II	(1)
	1447[a]	Protein; $\delta(CH_2)$ of sesquiterpenes	(1), (2)
	1412[a]	Protein	
	1346	COO–symmetric stretching vibrations of fatty acids and amino acid	(1)
	1242[a]	Asymmetric phosphate; amide III (C–N stretching of α-helical proteins)	(1)
	1161[a]	Carbohydrate; stretching vibrations of hydrogen-bonding C–OH groups (found in serine, threonine and tyrosine residues of cellular proteins); cellulose	(1), (3)
	1107[a]	Symmetric phosphate; ν(CO), ν(CC) ring (polysaccharides, pectin)	(1)
	1038[a]	ν(CC) skeletal *cis* conformation, $\nu(CH_2OH)$; Galactanν(CO) stretching coupled with C–O bending;	(1), (2)
	984	Protein phosphorylation; $\omega(CH_2)$ of monoterpenes	(1), (2)
	949[a]	Protein phosphorylation	(1), (3)
Site 3	1771	Lipid; fatty acid esters	(1)
	1732	Lipid; fatty acid esters; hemicellulose	(1), (3)
	1701	Lipid; fatty acid esters	(1)
	1632	Amide I; pectin	(1), (3)
	1585	Amide I	(1)
	1516[b]	Amide II	(1)
	1454[a]	Protein; $\delta(CH_2)$ of tetraterpenes	(1), (2)
	1416[a]	Protein	(1)
	1369	COO–symmetric stretching vibrations of fatty acids and amino acid; $\delta_{sym}(CH_3)$ sesquiterpenes	(1), (3)
	1308	Amide III	(1)
	1246[a]	Amide III (C–N stretching of α-helical proteins)	(1)
	1207	Asymmetric phosphate	(1)
	1165[a]	Carbohydrate; cellulose	(1), (3)
	1103[a]	Symmetric phosphate	(1)
	1042[a]	Symmetric PO_2 stretching in RNA and DNA;	(1)
	953[a]	Protein phosphorylation	(1)

ν: stretching, δ: deformation. [a] Loose correlation with other polluted site. [b] Exact correlation with other polluted site. References: (1) Movasaghi *et al.*, 2008;[47] (2) Schulz and Baranska, 2007;[36] (3) Stuart, 2004.[23]

associated with terpenes[36] were discovered at both sites (1447 cm^{-1} in Site 2 leaves, 1369 and 1454 cm^{-1} in Site 3 leaves). Several terpenes, particularly carotenoids are known to function as scavengers of ROS,[37] implying that leaves from polluted sites may have been exposed to higher ROS levels, possibly as a result of increased pollution exposure. Segregation from the rural control site (Site 1) was markedly greater for Site 3 leaves, implying a stronger effect of the urban exposure (Site 3) on leaf biochemistry than highway exposure (Site 2). Interestingly, there was no significant difference using one-way ANOVA (see ESI Table S1†) between the average Fv/Fm values from the three field sites ($P = 0.287$), indicating no discernible differences in the levels of stress experienced by plants at the different sites using this technique.

O_3 fumigation induces dose-dependent change in the spectral signature

Spectral datasets from O_3-free air- and O_3-fumigated (150 ppb and 300 ppb O_3) *A. pseudoplatanus* leaves were compared using multivariate analyses in order to derive biomarkers of controlled O_3 exposure. Following PCA-LDA transformation of pre-processed datasets, the three treatments segregated completely into distinct clusters (Fig. 2a). Segregation appeared to be predominantly in LD1, in concentration-dependent manner. A linear mixed effects model fit by REML revealed a significant effect of O_3 on LD1 values ($P = 0.003$). The cluster vectors plot (Fig. 2b) revealed substantial spectral segregation between the O_3 treatments and the control O_3-free air treatment across the biochemical fingerprint region. Similar changes were observed in both O_3 treatments and were generally more substantial in 300 ppb O_3-fumigated leaves this being indicative of a concentration-dependent response to O_3. Alterations were detected in several molecules (Table 3), and were highly prominent in lipid, amides, and proteins (1701, 1520, and 1458 cm^{-1}, respectively) suggesting possible damage to cell membranes and protein structures resulting from the generation of ROS by O_3. This is consistent with oxidative damage as the primary mode of O_3 toxicity in plants.[11]

Biotic stresses induce similar changes in the spectral signature

Spectral datasets from healthy (control) leaves of *A. pseudoplatanus* and those exhibiting two levels of *R. acerinum* infection (1–5 spots, and ≥10 spots) were compared using multivariate analyses. Following PCA-LDA transformation of pre-processed datasets, the three categories segregated completely into distinct clusters (Fig. 3a). As with O_3 treatment, segregation was predominantly in LD1, in a dose-dependent manner. A linear mixed effects model fit by REML revealed a significant effect of *R. acerinum* infection on LD1 values ($P < 0.001$). The cluster vectors plot (Fig. 3b) reveals substantial spectral segregation between the two infection levels and the uninfected control leaves across the biochemical fingerprint region. Strong alterations were detected in several molecules (Table 3), including amides, lipids, and proteins. Alterations to lipid may reflect ROS damage to cell membranes, which are generated in defence against pathogens *via* the oxidative burst mechanism.[38] In this case, ROS may be employed by the immune system as executioners of either the pathogen or the host cell.[39] Interestingly, leaf galls also

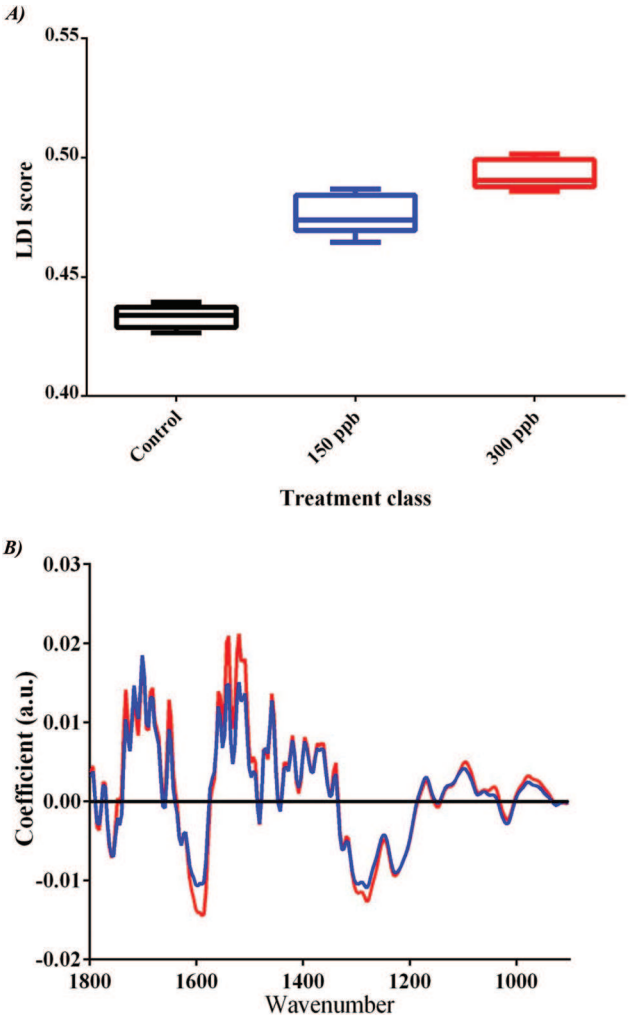

Fig. 2 (A) Box plot of PCA-LDA scores plot in one dimension derived from *A. pseudoplatanus* leaf tissue fumigated with either O_3-free air (black) or O_3 (blue, 150 ppb; red, 300 ppb) for seven hours over three days at two treatment concentrations, in addition to a control. (B) Cluster vectors plot by PCA-LDA indicating wavenumber basis for segregation following fumigation of *A. pseudoplatanus* leaf tissue with O_3. Each treatment (blue, 150 ppb; red, 300 ppb) was compared to the control (black, O_3-free air). The magnitude of the cluster vector peak or trough is proportional to the extent of biochemical alteration compared to the air control.

induced a highly significant effect on LD1 values (Welch two-sample *T*-test, $P < 0.001$), and the signature of alterations was almost identical to *R. acerinum* across the biochemical fingerprint region (see ESI Fig. S2, Table S2†), implying that the patterns observed are representative of a non-specific immune response.

Conserved changes in spectral signature between sampling sites, O_3, and biotic stresses

While it is important to note that our proposed mechanistic explanations for spectral alterations are largely speculative, conserved changes between different sites and stressors imply similar modes of action. The pseudospectra of the leaves exposed to the model abiotic and biotic stresses (O_3 and pathogen-infection, respectively) appear to be strikingly similar, particularly in the upper half of the spectrum (lipid, amide and protein regions). Many of these common elements also appear in the comparison between sites exposed to different vehicular

Table 3 ATR-FTIR spectroscopy distinguishing wavenumbers as shown in cluster vectors plot for *A. pseudoplatanus* leaf tissue exposed to abiotic (O_3 fumigation) and biotic stressors (tar spot infection). The most important wavenumbers responsible for segregation from the respective control leaves are shown, along with their tentative chemical assignments

Stressor	Wavenumber (cm^{-1})	Tentative assignment(s)	Reference(s)
Ozone	1759	Lipid	(1)
	1755	Lipid	(1)
	1701	Lipid; bases; fatty acid esters	(1)
	1651	Amide I; pectin	(1), (3)
	1597	Amide I; C=N, NH_2 adenine	(1)
	1589	Amide I; ring C–C stretch of phenyl	(1)
	1558	Amide II; ring base	(1)
	1520	Amide II	(1)
	1458	Proteins; $\delta_{as}CH_3$	(1)
	1373	COO–symmetric stretching vibrations of fatty acids and amino acid	(1)
	1366	COO–symmetric stretching vibrations of fatty acids and amino acid	(1)
	1281	Amide III	(1)
	1227	Asymmetric phosphate; ν_{as}(C–O–C) of geranyl acetate (acyclic monoterpene)	(1), (2)
	1099	Symmetric phosphate	(1)
	1169	Carbohydrate	(1)
	1096	Symmetric phosphate	(1)
	976	Protein phosphorylation	(1)
Tar spot	1724	Lipid; fatty acid esters	(1)
	1701	Lipid; fatty acid esters	(1)
	1686	Amide I	(1)
	1632	Amide I; C=C uracil, C=O; pectin	(1), (3)
	1628	Amide I	(1)
	1597	Amide I; C=N, NH_2 of adenine	(1)
	1593	Amide I	(1)
	1539	Amide II	(1)
	1458	Proteins; $\delta_{as}CH_3$	(1)
	1373	COO–symmetric stretching vibrations of fatty acids and amino acid	(1)
	1308	Amide III	(1)
	1304	Amide III	(1)
	1246	Amide III; PO_2 asymmetric	(1)
	1107	Symmetric phosphate; ν(CO), ν(CC) ring (polysaccharides, pectin)	(1)
	1011	Glycogen; $CH_{\alpha,\alpha'}$ out-of-plane bending and C_α=$C_{\alpha'}$ torsion	(1)

ν: stretching, δ: deformation. References: (1) Movasaghi *et al.*, 2008;[47] (2) Schulz and Baranska, 2007;[36] (3) Stuart, 2004.[23]

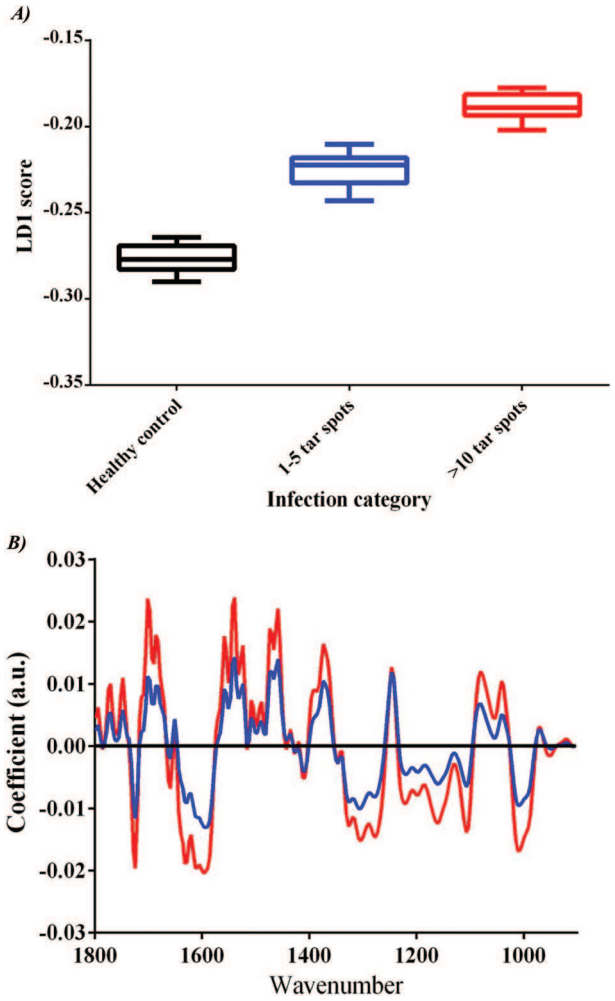

Fig. 3 (A) Box plot of PCA-LDA scores in one dimension derived from *A. pseudoplatanus* leaf tissue displaying different levels of *R. acerinum* infection (black, healthy leaves; blue, 1–5 tar spots; red, ≥10 tar spots). (B) Cluster vectors plot by PCA-LDA indicating wavenumber basis for segregation between *A. pseudoplatanus* leaf tissue samples displaying different levels of *R. acerinum* fungal infection. Each infection class (blue, 1–5 tar spots; red ≥10 spots) was compared to the background healthy control leaves (black). The magnitude of the cluster vector peak or trough is proportional to the extent of biochemical alteration compared to the background healthy control.

exhaust exposures. For example, in the upper half of the spectrum, alterations to lipid (1701 cm^{-1}), and Amide I and II (~1630–1580 cm^{-1}) appear to be induced by both model stresses and urban exposure (Site 3), and may be indicative of changes to cell membranes and proteins, implying possible degradation of these structures. Furthermore, the pseudospectra associated with O_3 and biotic stress appears to possess analogous peaks to those associated with terpenes (ROS scavengers) in leaves from polluted sites, Sites 2 and 3 (*e.g.*, 1373 cm^{-1} in both model stresses). These common alterations may result from oxidative damage within leaves, as this is a common mode of action of air pollutants and is also a consequence of pathogen infection *via* the oxidative burst defence mechanism. Interestingly, pseudospectral alterations similar to those induced by the model stress used in the present study have also been reported in bacterial cells exposed to UV-A, which also induces ROS production.[40] Our observation that Site 3 pseudospectra possess many alterations detected in response to the model stresses used in this study further implies that these represent sub-lethal effects of pollution exposure. Other areas of the spectra showed no obvious similarities between the different stressors and sites, and these alterations are likely more reflective of sources of variation not directly associated with pollution.

4. Conclusions and future work

The societal value of tree species is already well-appreciated for their aesthetic and psychological value,[41] as well as their capacity to sequester air pollutants.[8,9] The present study has demonstrated that biospectroscopy can unlock yet another benefit of urban trees: their utility as biological monitoring stations, from which complex biochemical data regarding the impacts of environmental pollutants can be acquired and scrutinised. This study identified key differences in spectral signatures of plants from environments in which they were exposed to different levels of vehicle pollution. Importantly, plant stress could not be detected using conventional monitoring techniques such as chlorophyll fluorescence (Fv/Fm) suggesting that biospectroscopy of sentinel species may provide new approach for monitoring pre-symptomatic effects. Interestingly, the identification of alterations in the spectral signature of *A. pseudoplatanus* that are common to ROS-inducing stresses provides putative biomarkers. Although the chemical identities of these biomarkers are yet to be verified with other techniques, their consistent appearance under different environmental stress conditions, both abiotic and biotic stresses, suggests they may serve as reliable and quantitative indicators of the stress levels of plants, which could be correlated with pollution exposure.

Biospectroscopy shows promise of being a powerful toolkit in environmental health monitoring.[21] Our results demonstrate that this toolkit can be applied to effectively utilise tree species as sentinel organisms. Correlated with conventional monitoring data and other biomarker approaches (*e.g.*, Trad-MCN assay),[42] large-scale studies across a range of differentially polluted sites taking into account additional variables such as synergistic effects,[2,43,44] or other sources of environmental variability (*e.g.*, soil nutrients, specific contaminants)[45,46] are now required to further validate this approach. Nevertheless, it is clear that pollution-specific biomarkers in plant sentinel species constitute an exciting new approach for environmental health monitoring.

Acknowledgements

We wish to thank Dawn Worrall and Geoff Holroyd for assistance with O_3 fumigation. We also wish to thank the Fairfield Association (Lancaster, UK) for their cooperation in the study.

References

1 P. H. Fischer, M. Marra, C. B. Ameling, G. Hoek, R. Beelen, K. de Hoogh, O. Breugelmans, H. Kruize, N. A. Janssen and D. Houthuijs, *Environ. Health Perspect.*, 2015, **123**, 697–704.
2 R. M. Harrison, *Pollution: Causes, Effects and Control*, Royal Society of Chemistry, 2001.
3 D. W. Dockery and P. H. Stone, *N. Engl. J. Med.*, 2007, **356**, 511–513.
4 G. Oberdörster, E. Oberdörster and J. Oberdörster, *Environ. Health Perspect.*, 2005, **1**, 823–839.
5 P. Georgiadis, J. Topinka, M. Stoikidou, S. Kaila, M. Gioka, K. Katsouyanni, R. Sram, H. Autrup and S. A. Kyrtopoulos, *Carcinogenesis*, 2001, **22**, 1447–1457.
6 A. Klumpp, W. Ansel, G. Klumpp, V. Calatayud, J. P. Garrec, S. He, J. Penuelas, A. Ribas, H. Ro-Poulsen, S. Rasmussen and M. J. Sanz, *Environ. Pollut.*, 2006, **139**, 515–522.
7 F. L. Martin, *Nat. Methods*, 2011, **8**, 385–387.
8 D. J. Nowak, D. E. Crane and J. C. Stevens, *Urban For. Urban Green.*, 2006, **4**, 115–123.
9 D. J. Nowak, S. Hirabayashi, A. Bodine and E. Greenfield, *Environ. Pollut.*, 2014, **193**, 119–129.
10 L. D. Claxton and G. M. Woodall, *Mutat. Res., Rev. Mutat. Res.*, 2007, **636**, 36–94.
11 J. N. Bell and M. Treshow, *Air Pollution and Plant Life*, John Wiley & Sons, Ltd, 2002.
12 A. Nadgórska-Socha, B. Ptasiński and A. Kita, *Ecotoxicology*, 2013, **22**, 1422–1434.
13 E. Navarro, A. Baun, R. Behra, N. B. Hartmann, J. Filser, A. J. Miao, A. Quigg, P. H. Santschi and L. Sigg, *Ecotoxicology*, 2008, **17**, 372–386.
14 R. Aina, L. Palin and S. Citterio, *Chemosphere*, 2006, **65**, 666–673.
15 A. S. Heagle, *Annu. Rev. Phytopathol.*, 1973, **11**, 365–388.
16 I. D. Leith and D. Fowler, *New Phytol.*, 1988, **108**, 175–181.
17 K. Maxwell and G. N. Johnson, *J. Exp. Bot.*, 2000, **51**, 659–668.
18 E. Schreck, C. Laplanche, M. Le Guédard, J. J. Bessoule, A. Austruy, T. Xiong, Y. Foucault and C. Dumat, *Environ. Pollut.*, 2013, **179**, 242–249.
19 J. Meireles, R. Rocha, A. C. Neto and E. Cerqueira, *Mutat. Res., Genet. Toxicol. Environ. Mutagen.*, 2009, **675**, 46–50.
20 J. Trevisan, P. P. Angelov, P. L. Carmichael, A. D. Scott and F. L. Martin, *Analyst*, 2012, **137**, 3202–3215.
21 B. E. Obinaju and F. L. Martin, *Environ. Pollut.*, 2013, **183**, 46–53.
22 J. G. Kelly, J. Trevisan, A. D. Scott, P. L. Carmichael, H. M. Pollock, P. L. Martin-Hirsch and F. L. Martin, *J. Proteome Res.*, 2011, **10**, 1437–1448.
23 B. H. Stuart, *Infrared Spectroscopy: Fundamentals and Applications*, John Wiley & Sons, Ltd, 2004.
24 M. S. Braiman and K. J. Rothschild, *Annu. Rev. Biophys. Biophys. Chem.*, 1988, **17**, 541–570.
25 M. J. Baker, J. Trevisan, P. Bassan, R. Bhargava, H. J. Butler, K. M. Dorling, P. R. Fielden, S. W. Fogarty, N. J. Fullwood, K. A. Heys, C. Hughes, P. Lasch, P. L. Martin-hirsch, B. Obinaju, G. D. Sockalingum, J. Sulé-Suso, R. J. Strong, M. J. Walsh, B. R. Wood, P. Gardner and F. L. Martin, *Nat. Protoc.*, 2014, **9**, 1771–1791.
26 X. Li, J. B. Zhang, B. Song, H. P. Li, H. Q. Xu, B. Qu, F. J. Dang and Y. C. Liao, *Phytopathology*, 2010, **100**, 183–191.
27 K. A. Heys, M. J. Riding, R. J. Strong, R. F. Shore, M. G. Pereira, K. C. Jones, K. T. Semple and F. L. Martin, *Analyst*, 2014, **139**, 896–905.
28 V. Llabjani, R. N. Malik, J. Trevisan, V. Hoti, J. Ukpebor, Z. K. Shinwari, C. Moeckel, K. C. Jones, R. F. Shore and F. L. Martin, *Environ. Int.*, 2012, **48**, 39–46.
29 M. Aja, M. Jaya, K. V. Nair and I. H. Joe, *Spectrochim. Acta Part A*, 2014, **120**, 534–541.
30 B. E. Obinaju, A. Alaoma and F. L. Martin, *Environ. Pollut.*, 2014, **192**, 222–231.
31 B. Ribeiro da Luz, *New Phytol.*, 2006, **172**, 305–318.
32 J. P. O'Connor, M. A. O'Connor, P. Ashe and S. Wistow, *Ir. Nat. J.*, 1999, **26**, 241–248.
33 D. R. Hoagland and D. I. Arnon, *The Water-culture Method for Growing Plants Without Soil, Circular*, California Agricultural Experiment Station, 2nd edn, 1950.
34 L. Delle Monache and R. B. Stull, *Atmos. Environ.*, 2003, **37**, 3469–3474.
35 C. M. Rico, J. R. Peralta-Videa and J. L. Gardea-Torresdey, *Appl. Spectrosc.*, 2015, **69**, 287–295.
36 H. Schulz and M. Baranska, *Vib. Spectrosc.*, 2007, **43**, 13–25.
37 L. Pérez-Rodríguez, *BioEssays*, 2009, **31**, 1116–1126.
38 P. Wojtaszek, *Biochem. J.*, 1997, **322**, 681–692.
39 M. A. Torres, J. D. Jones and J. L. Dangl, *Plant Physiol.*, 2006, **141**, 373–378.
40 M. J. Riding, J. Trevisan, C. J. Hirschmugl, K. C. Jones, K. T. Semple and F. L. Martin, *Environ. Int.*, 2012, **50**, 56–65.
41 R. A. Fuller, K. N. Irvine, P. Devine-Wright, P. H. Warren and K. J. Gaston, *Biol. Lett.*, 2007, **3**, 390–394.
42 E. Ceretti, C. Zani, I. Zerbini, G. Viola, M. Moretti, M. Villarini, L. Dominici, S. Monarca and D. Feretti, *Chemosphere*, 2015, **120**, 221–229.
43 A. H. Chappelka and L. J. Samuelson, *New Phytol.*, 1998, **139**, 91–108.
44 S. Warrington, D. A. Cottam and J. B. Whittaker, *Oecologia*, 1989, **80**, 136–139.
45 B. E. Obinaju, C. Graf, C. Halsall and F. L. Martin, *Environ. Pollut.*, 2015, **192**, 222–231.
46 H. J. Butler, M. R. McAinsh, S. Adams and F. L. Martin, *Anal. Methods*, 2015, **7**, 4059–4070.
47 Z. Mouasaghi, S. Rehman and D. I. ur Rehman, *Appl. Spectrosc. Rev.*, 2008, **43**, 134–179.